



biblio.ugent.be

The UGent Institutional Repository is the electronic archiving and dissemination platform for all UGent research publications. Ghent University has implemented a mandate stipulating that all academic publications of UGent researchers should be deposited and archived in this repository. Except for items where current copyright restrictions apply, these papers are available in Open Access.

This item is the archived peer-reviewed author-version of:

Title: Single-step formation degradable intracellular biomolecule microreactors

Authors: Dierendonck M., De Koker S., De Rycke R., Bogaert P., Grooten J., Vervaet C., Remon J.P., De Geest B.G.

In: ACS Nano, 5(9), 6886-6893 (2011)

Optional: link to the article

To refer to or to cite this work, please use the citation to the published version:

Authors (year). Title. *journal Volume(Issue)* page-page. Doi 10.1021/nn200901g

A single step process for the synthesis of antigen laden thermosensitive Microparticles

Bruno G. De Geest,^a Stefaan De Koker,^b Yves Gonnissen,^{ac} Liesbeth J. De Cock,^a Johan Grooten,^b Jean Paul Remon^a and Chris Vervaeke^a

- a Laboratory of Pharmaceutical Technology, Department of Pharmaceutics, Ghent University, Ghent, Belgium
- b Department of Biomedical Molecular Biology, Ghent University, Ghent, Belgium
- c SEPS Pharma, Tongeren, Belgium

Recent insights in vaccine delivery point out a distinct benefit for antigen to be delivered in a microparticulate form to professional antigen presenting cells. Encapsulation technology to produce antigen laden microparticles often requires complex handlings involving the use of organic solvents, chemical reactivity and/or high shear forces. These issues impair the practical and economical feasibility of such delivery systems. In this paper, we introduce a novel concept for the encapsulation of antigen within microparticles, making use of the lower critical solution temperature (LCST) behavior of a thermosensitive carrier polymer. Particle fabrication and characterization is demonstrated as well as their uptake by dendritic cells.

Introduction

Current insights in immunology, especially in how the immune system recognizes pathogens and translates this into the induction of the appropriate adaptive immune response, pave the way for a more rational vaccine design.^{1–4} Besides the choice of the antigen and the addition of immunopotentiators, it has become clear that also the way this antigen is delivered to the immune system dramatically affects the outcome of immunisation. Generally speaking, at least three major advantages of microparticulate antigen delivery can be defined. First, encapsulation in particles with sizes varying from 1–10 μ m increases, due to cell type dependent size limitations, their uptake by professional antigen presenting cells such as dendritic cells (DC's). Second, uptake of antigens in a particulate form appears to strongly augment antigen presentation via MHC I (major histocompatibility complex I), a feature hardly achievable when using soluble antigens. MHC I mediated presentation is crucial for the induction of CD8 cytotoxic T cell responses, which can recognize and kill virally infected or malignant cells. Third, the potency of an immune response is strongly increased when both

antigen and adjuvant are co-delivered to the same intracellular compartment of the same antigen presenting cell. This means that strategies allowing an efficient co-encapsulation of antigen and immunopotentiator in the same particle could strongly enhance vaccine efficiency. These requirements for improved vaccination are not met by traditional vaccination strategies which commonly involve the use of aluminium salts or oil/water emulsions, merely generating a depot effect.

Drug delivery scientists have developed a myriad of particulate delivery systems to encapsulate antigens in micro- and nanoparticles to enhance the induced immune response.^{5–13} The main drawback of these approaches is most often the use of organic solvents, harsh chemical reactions, long lasting shear forces and the involvement of a multitude of batch operation steps before obtaining the final antigen formulation. These issues severely limit the batch-to-batch reproducibility of the developed delivery system, while the complexity of the process hampers the feasibility of any clinical trial or large scale production. Therefore, there is a clear need for single step processes which can generate stable, antigen-laden particles with such dimensions (i.e. sub-10 μ m) that they are efficiently taken up by antigen presenting cells.

In this paper, we report on a simple yet efficient method to produce antigen-laden microparticles, which are stable both in dry state as well as in water in physiological conditions. The novelty of the concept lies in the use of a lower critical solution temperature (LCST) behaving polymer as excipient in combination with spray drying as particle producing technique. Below the LCST of the polymer excipient, the aqueous feed is a clear antigen/polymer solution, while the obtained spray dried microparticles form a colloidal stable suspension in aqueous medium at physiological temperature (i.e. 37 $^{\circ}$ C; above the LCST of the polymer excipient).

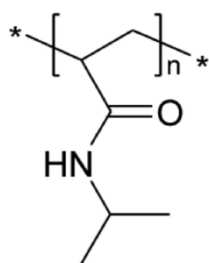


Fig. 1 Chemical structure of polyNIPAA.

In this study, we use poly(N-isopropylacrylamide) (poly-NIPAA) as model LCST polymer. The chemical structure of polyNIPAA is shown in Fig. 1, while Fig. 2 schematically represents the desired behavior of the microparticles in aqueous medium at different temperatures. PolyNIPAA is the classic example of a polymer exhibiting LCST behavior.^{14–19} This means that below a certain temperature (i.e. the LCST; 32 °C for polyNIPAA) the polymer is hydrated and fully water soluble, while upon increasing temperature the entropy of the solvent molecules becomes that high that the polymer is no longer hydrated and becomes hydrophobic. The consecutive process of chain collapse and aggregation, forming microparticles can be used to encapsulate a drug payload.

Experimental

Materials

Ovalbumin (OVA; grade III), fluorescein isothiocyanate (FITC) and poly(N-isopropylacrylamide) (polyNIPAA; Mw = 20–25 kDa) were purchased from Sigma-Aldrich. Mannitol (C* Mannidex 16700) was donated by Cerestar. FITC labeled OVA was synthesized by mixing OVA and FITC in a borate buffer at pH 8.5 followed by extensive dialysis and lyophilisation.

Microparticle spray drying

An aqueous solution of OVA, polyNIPAA and mannitol (OVA/polyNIPAA/mannitol ratio: 1/5/15, total solid content: 4.0% w/w) was prepared. Spray drying of this solution was performed in a lab-scale spray dryer, type B290 (Bucchi). The solution was fed to a two-fluid nozzle (diameter 0.7 mm) at the top of the spray dryer. In addition, the spray dryer operated in co-current air flow. This aqueous solution was spray dried according to the process parameters shown in Table 1.

The spray dried particles were collected in a reservoir attached to a cyclone, cooled down to room temperature and stored in sealed vials (room temperature, ambient relative humidity) prior to their characterisation and further use. Fluorescent microparticles were prepared using a mixture of 180 mg OVA and 20 mg of FITC-OVA.

Bone-marrow derived DCs (BM-DCs)

Female C57BL/6 mice were purchased from Janvier (Le Genest

Saint Isle, France) and housed in a specified pathogen-free facility in micro-isolator units. Dendritic cells were generated using a modified Inaba protocol.²⁰ Two to six months C57BL/6 mice were sacrificed and bone marrow was flushed from their femurs and tibias. After lysis of red blood cells with ACK lysis buffer (BioWhittaker, Walkersville, MD), granulocytes and B cells were depleted using Gr-1 (Pharmingen) and B220 (Pharmingen) antibodies, respectively, and low-toxicity rabbit complement (Cedarlane Laboratories Ltd., Hornby, Ontario, Canada). Cells were seeded at a density of 2×10^5 cells ml⁻¹ in 175 cm² Falcon tubes (Becton Dickinson) in DC medium (RPMI 1640 medium containing 5% LPS-free FCS, 1% penicillin/streptomycin, 1% L-glutamine and 50 mM β -mercaptoethanol) containing 10 ng ml⁻¹ IL-4 and 10 ng ml⁻¹ GM-CSF (both from Peprotech, Rock Hill, NJ). After two days and again after four days of culture, the non-adherent cells were centrifuged, resuspended in fresh medium and replated to the same Falcon tubes. On the sixth day, non-adherent cells were removed and fresh medium containing 10 ng ml⁻¹ GM-CSF and 5 ng ml⁻¹ IL-4 was added. On day 8 of culture, non-adherent cells were harvested and used for the experiments.

Uptake and cytotoxicity assays

Cells were washed, fixed with 4% paraformaldehyde, stained with alexa 488 cholera toxin subunit B (5mg ml⁻¹, Molecular Probes) and visualized by confocal microscopy. Nuclei were stained with DAPI (1 mM). Flow-cytometry samples were measured on a FACSCalibur (BD) flow cytometer and analyzed using CellQuestTM software.

Cytotoxicity was assessed using a classical p-nitrophenyl phosphate (pNPP) cell viability assay. Human dermal fibroblasts (ATCC CRL-2522) were seeded in a 96-well plate at 2.5×10^3 cells per well and incubated for 6 h with the spray dried microparticles at different concentrations followed by medium renewal and a further 2 days of culturing. Subsequently, the cell medium was removed and 50 μ l of pNPP assay solution was added followed by incubation at 37 °C and 5% CO₂. After 2 h the reaction was stopped by addition of NaOH and the absorbance was measured spectrophotometrically at 405 nm.

Characterization

Optical microscopy images were recorded on a Nikon EZ-C1

confocal microscope. Scanning electron microscopy (SEM) images were recorded at 5 kV acceleration voltage on a Quanta FEG FEI scanning electron microscope applying a gold/palladium sputtering prior to SEM imaging. Dynamic light scattering was performed on a Malvern Nanosizer. Protein content was measured by Bio-Rad Protein Assay. ATR-FTIR spectra were recorded on Biorad 930C apparatus using the Golden Gate accessory (diamond crystal). 32 scans were performed at a resolution of 4 cm⁻¹.

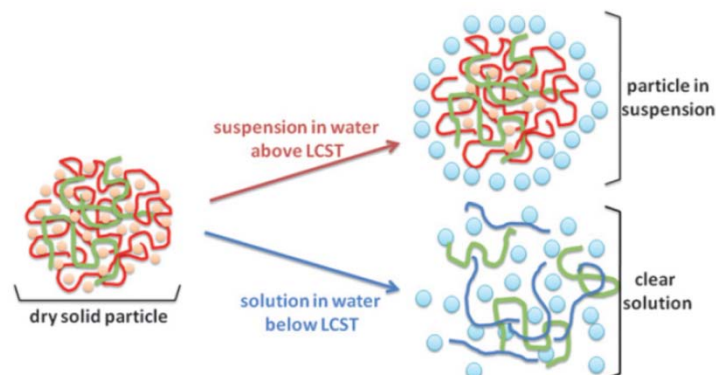


Fig. 2 Schematic representation of the physicochemical behavior of the thermosensitive antigen-laden microparticles. In dry state the microparticles consist of collapsed polyNIPAA molecules (red curves) encapsulating the OVA (green curves) with mannitol (orange spots) as additional excipient distributed throughout the volume of the particles. Upon suspension in water (light blue discs) above the LCST of polyNIPAA, the polyNIPAA molecules retain their collapsed formulation still encapsulating the OVA. The low molecular weight mannitol remains partly bound to the particles and partly goes into solution. When the temperature of the aqueous medium is below the LCST of the polyNIPAA, the polyNIPAA chains are hydrated and all components go in solution.

Table 1 Process conditions during spray drying in the lab scale spray dryer, type B290

Process parameters Process

Inlet drying air temperature 130 °C

Outlet drying air temperature 65 °C

Drying air gas rate 35 m³ h⁻¹

Atomising nitrogen pressure 0.3 bar

Results and discussion

In our set-up a clear solution of polyNIPAA, ovalbumin (OVA) and mannitol was fed at room temperature (i.e. below the LCST of the polyNIPAA) to a bench top spray dryer. Mannitol is a polyol that is often used as excipient in pharmaceutical applications to stabilize sensitive drug molecules and due to its relatively

low hydroscopicity which prevents spray-dried microparticles from sticking. OVA is a 43 kDa protein derived from chicken egg white and is commonly used as model antigen in mechanistic immunological research.

The obtained product (process yield: 39%) was a white powder with a mean particle diameter of 4.5 μ m as determined by image analysis. The particle morphology was assessed by scanning electron microscopy (SEM). The corresponding images are shown in Fig. 3A-B and reveal a rather irregular shape of the microparticles, typical for polymer-based spray dried formulations.

The powder was readily soluble in water at room temperature (i.e. below the LCST of polyNIPAA) but formed a turbid suspension when the powder was reconstituted with water heated above the LCST of polyNIPAA. Addition of mannitol to the feed solution prior to spray drying was required in order to allow redispersion of the powder in water above the LCST of polyNIPAA. In absence of mannitol or when using another excipient (e.g. maltodextrin), large aggregated clumps were formed when attempting to redisperse in water above the LCST of polyNIPAA. The temperature-dependent behavior of the produced microparticles was monitored by measuring the transmittance of UV/VIS light as a function of temperature and the recorded curves are shown in Fig. 4. The inset of Fig. 4 shows the transmittance of polyNIPAA in water as a function of the temperature. A steep decrease in transmittance is observed at around 32 $^{\circ}$ C, which is well known for polyNIPAA. The transmittance of the microparticles suspended in water at 40 $^{\circ}$ C (blue curve with cubic symbols going from right to left) indicates a moderately turbid solution. Upon decreasing temperature the transmittance increases until a clear solution is obtained at around 31 $^{\circ}$ C. Interestingly, the shift in transmittance occurs more gradually than in the case of pure poly-NIPA, which is likely due to physico-chemical interactions such as H-bonding and hydrophobic interactions, between the polyNIPA and the OVA and mannitol, respectively. The formation of H-bonding between the NH group of polyNIPA and carboxylic acids is well known.^{21,22} This is expected as well in our system as OVA contains many carboxylic acid bearing aminoacids. Moreover, hydrophobic interactions with more hydrophobic domains in OVA are likely to occur as well. Since in our case we are dealing with a complex mixture, it is difficult

to elucidate the exact contribution of the respective interactions.

However, ATR-FTIR spectroscopy shows that the intensity ratio of the amide I (C=O ; ν 1650 cm^{-1}) to the amide II peak (NH ; ν 1545–1516 cm^{-1}) was significantly higher for the spray-dried microparticles compared to the native polyNIPAA and OVA. According to literature this is indicative of the presence of H-bond and/or hydrophobic interactions between the different components within the spray-dried microparticles.²²

When the same solution is reheated to 40 °C (red curve with circular symbols going from left to right), as expected, a shift in transmittance is observed at around 32 °C but a much lower transmittance at 40 °C is observed as compared to the transmittance of the starting suspension at 40 °C. When again the temperature is decreased (black curve with triangular symbols going from right to left), the transmittance follows an identical track as the previous heating track (red curve with circular symbols). Also, these two curves (red and black) show a more gradual shift in transmittance than the pure polyNIPAA, again most likely due to interactions with the OVA and mannitol, respectively. The observed lower transmittance of the suspension obtained upon reheating as compared to the transmittance of the original starting suspension at 40 °C is further confirmed visually, as shown in Fig. 4 with photographs of the liquids at different stages of the heating/cooling cycle. A moderately turbid suspension upon redispersing of the powder in water at 40 °C, a clear solution at room temperature and a strongly turbid solution upon reheating to 40 °C are observed. The reason for this behavior is revealed by SEM and dynamic light scattering showing a much lower particle size (i.e. 120 ± 34 nm) of the reheated suspension (Fig. 3C) compared to the original starting suspension (Fig. 3A-B). For the same mass of materials this corresponds to a much higher amount of particles in case of the reheated suspension and thus a decrease in light transmittance.

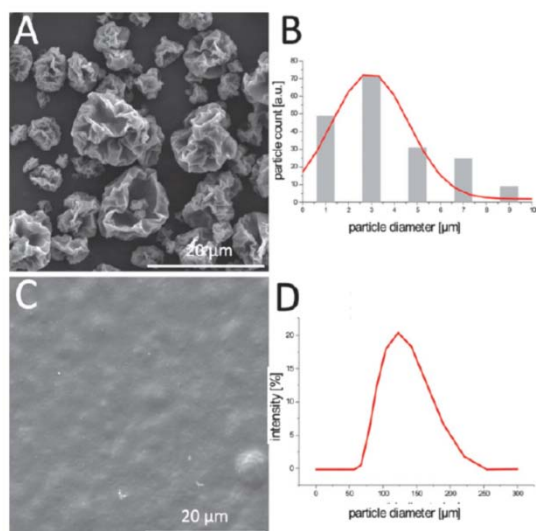


Fig. 3 Scanning electron microscopy (SEM) images of the spray dried microparticles (A) as such after spray drying and (C) after a reheating cycle. (B) and (D) show the corresponding size distribution curves of (A) spray dried microparticles as measured by image analysis and (C) reheated particles as measured by dynamic light scattering (DLS).

The particle disassembly upon temperature decrease was imaged by optical microscopy. A drop of heated microparticle suspension was put onto a coverslip under a confocal microscope and snapshots were taken at regular time intervals while the droplet was cooled spontaneously by interaction with the ambient environment. As shown in Fig. 5, the particle (the darkish color is most likely due to the non-hydrated interior of the particle) gradually decreases in size until it is completely dissolved.

The encapsulation efficiencies in dry and wet state were determined separately. Encapsulation of OVA in the dry powder was determined by dissolving a known amount of powder at room temperature and measuring the amount of protein by Bradford protein assay,²³ revealing an encapsulation efficiency of 48 ± 6%, relative to the protein concentration in the feed stream prior to spray drying. Release of OVA from the microparticles when suspended above the LCST of polyNIPA was measured by filtering the microparticle suspension at 40 °C and measuring the amount of protein in the filtrate by Bradford protein assay. No protein was detected in this filtrate showing excellent retention of the protein within the microparticles upon suspension in water above the LCST. Confocal microscopy (Fig. 6A) and flow cytometry (Fig. 6B) allowed to assess the uptake of the particles by bone marrow derived mouse dendritic cells (DCs). This cell type was chosen to

study microparticle internalization as DCs are professional antigen presenting cells and thus the primary target cells for vaccine delivery systems. For this purpose, fluorescent microparticles were produced by adding an amount of fluorescein isothiocyanate-labeled ovalbumin (FITC-OVA) to the feed solution prior to spray drying. The thus obtained powder had a yellowish color and was green-fluorescent upon illumination with 488 nm light. During addition of the microparticles to the cultured DCs, care was taken in order to ensure a constant temperature of 37 °C of both the microparticle suspension and the cell medium, in order to avoid dissolution of the microparticles due to a temperature drop. The confocal image is shown in Fig. 6A and is recorded 4 h after the incubation of the DCs with the microparticle suspension. The cell nuclei were stained blue with DAPI and the cell membrane was stained red with Alexa594 labeled cholera toxin B subunit. In this image, it is clear that the green fluorescent microparticles are efficiently taken up by the DCs. This was further confirmed by flow cytometry (Fig. 6B)

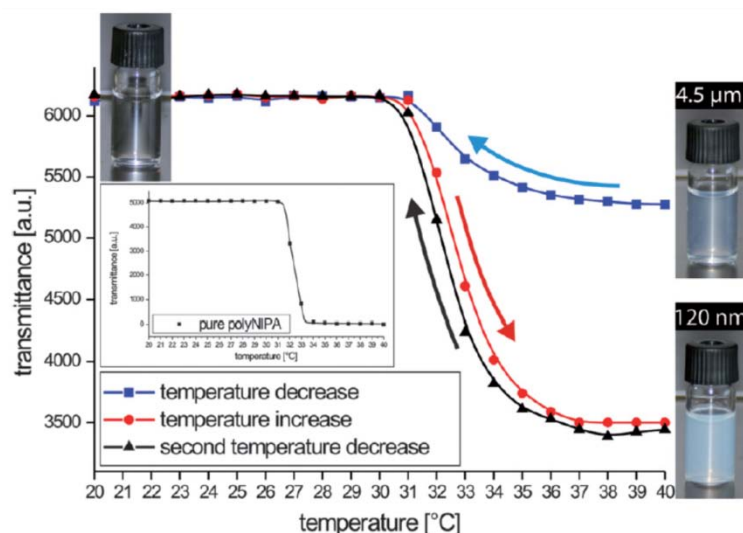


Fig. 4 Transmittance plots of the microparticle suspension recorded at decreasing temperature (●), followed by increasing temperature (○) and again decreasing temperature (△). The inset shows the transmittance plot of pure polyNIPAA. Next to the curves, photographs are shown of the corresponding liquids.

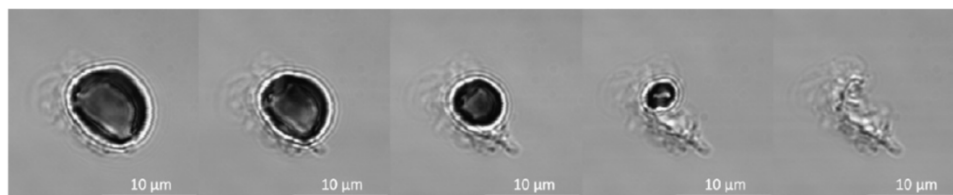


Fig. 5 Optical microscopy snapshots of the temperature induced dissolution of the spray-dried microparticles. A drop of microparticle suspension at a temperature above the LCST of polyNIPAA was placed on a cover slip imaged by a confocal microscope at room temperature. The effect of the gradual decrease of the aqueous medium towards room temperature was monitored by taking snapshots at 5 s time intervals.

showing an increasing shift in fluorescence with the concentration of added microparticles. Cytotoxicity of the microparticles was assessed on a human dermal fibroblast cell line by a common pNPP cell viability assay. This cell type was chosen because it is abundantly present subcutaneous (i.e. a common administration route for vaccine delivery). The graphs shown in Fig. 6C show no detectable cytotoxicity of the microparticles at moderate concentrations and only a slight decrease in cell viability in the case of microparticle concentrations as high as 4 mg ml⁻¹.

Conclusions

In this paper, we have demonstrated a simple and efficient method for producing antigen laden microparticles with dimensions allowing uptake by antigen presenting cells. Our main concept is the use of a difference in physicochemical conditions (i.e. temperature in this case) between the spray drying feed stream (room temperature of 25 °C) and the final medium in which the particles are suspended (i.e. physiological conditions exhibiting a temperature of 37 °C). Therefore we used the LCST phenomenon, allowing the production (starting from a clear feed solution) of solid microparticles, which can be resuspended at temperatures above the LCST of the carrier polymer and readily dissolve below the LCST. Our approach has two main assets. The first one is the simplicity of our production process. Spray drying is a continuous, single-step processing technique,^{24,25} which can be scaled up easily, allowing large-scale industrial production of our antigen laden microparticles. The second asset is the possibility to incorporate an almost unlimited variety of additional components within the microparticles. This allows simultaneous incorporation of additional adjuvants into the microparticles, making this technology a general platform for the production of vaccines, thus allowing one to modulate the induced immune response by varying the microparticles' content. Also, additional excipients can be easily incorporated, which might further enhance antigen stability in a dry formulation.

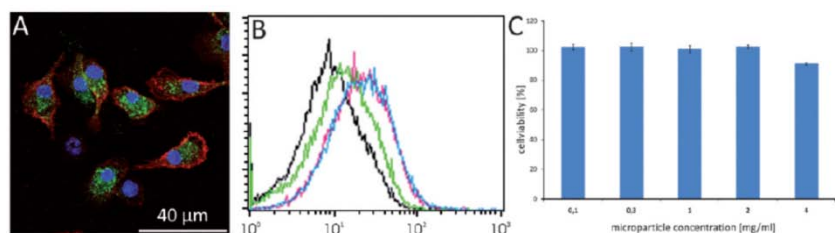


Fig. 6 (A) Confocal microscopy image of bone marrow derived dendritic cells (DC's) incubated with the microparticles. The cell nuclei were stained blue with DAPI, the cell membrane was stained red with Cy5 labeled cholera toxin B subunit and the microparticles were fluorescent green. (B) Corresponding flow cytometry histogram of dendritic cells incubated with different amounts of fluorescent microparticles. (C) Cell viability data of the microparticles determined using a standard pNPP assay.

We are fully aware of the fact that poyNIPAA is not biodegradable and thus antigen release will not spontaneously occur under physiological conditions. However, with this explorative study, we aimed to demonstrate a proof-of-concept (using a model LCST polymer). Further studies will focus on the use of biodegradable LCST polymers (e.g. polyhydropropylmethacrylamide-dilactate (polyHPMA-lac2) which consist of polyHPMA with pending lactate groups).²⁶ This polymer, having two lactate moieties substituted on the hydroxyl group of each repeating unit, has an LCST of 15 °C which increases to 62 °C upon hydrolysis of a lactate unit. This approach would allow the production of microparticles which are stable above the LCST but which gradually dissolve due to hydrolysis of the LCST polymer.

Acknowledgements

B.D.G. acknowledges the FWO Vlaanderen for a postdoctoral scholarship. Filip Du Prez and Bart Derveaux are thanked for transmittance experiments. Joachim Zephirin is thanked for practical assistance.

References

- 1 A. M. Mowat, Nat. Rev. Immunol., 2003, 3, 331–341.
- 2 P. Ricciardi-Castagnoli and F. Granucci, Nat. Rev. Immunol., 2002, 2, 881–888.
- 3 Y. van Kooyk and T. B. H. Geijtenbeek, Nat. Rev. Immunol., 2003, 3, 697–709.
- 4 C. R. E. Sousa and R. N. Germain, J. Exp. Med., 1995, 182, 841–851.
- 5 R. Langer and D. A. Tirrell, Nature, 2004, 428, 487–492.

- 6 D. T. O'Hagan and N. M. Valiante, *Nat. Rev. Drug Discovery*, 2003, 2, 727–735.
- 7 B. G. De Geest, S. De Koker, K. Immesoete, J. Demeester, S. C. De Smedt and W. E. Hennink, *Adv. Mater.*, 2008, 20, 3687.
- 8 B. G. De Geest, S. De Koker, G. B. Sukhorukov, O. Kreft, W. J. Parak, A. G. Skirtach, J. Demeester, S. C. De Smedt and W. E. Hennink, *Soft Matter*, 2009, 5, 282.
- 9 B. G. De Geest, C. Dejumat, M. Prevot, G. B. Sukhorukov, J. Demeester and S. C. De Smedt, *Adv. Funct. Mater.*, 2007, 17, 531–537.
- 10 B. G. De Geest, C. Dejumat, G. B. Sukhorukov, K. Braeckmans, S. C. De Smedt and J. Demeester, *Adv. Mater.*, 2005, 17, 2357–2361.
- 11 B. G. De Geest, N. N. Sanders, G. B. Sukhorukov, J. Demeester and S. C. De Smedt, *Chem. Soc. Rev.*, 2007, 36, 636–649.
- 12 B. G. De Geest, R. E. Vandenbroucke, A. M. Guenther, G. B. Sukhorukov, W. E. Hennink, N. N. Sanders, J. Demeester and S. C. De Smedt, *Adv. Mater.*, 2006, 18, 1005.
- 13 S. De Koker, B. G. De Geest, C. Cuvelier, L. Ferdinande, W. Deckers, W. E. Hennink, S. De Smedt and N. Mertens, *Adv. Funct. Mater.*, 2007, 17, 3754–3763.
- 14 I. Tokarev and S. Minko, *Soft Matter*, 2009, 5, 511–524.
- 15 L. A. Lyon, Z. Y. Meng, N. Singh, C. D. Sorrell and A. S. John, *Chem. Soc. Rev.*, 2009, 38, 865–874.
- 16 X. Z. Zhang, X. D. Xu, S. X. Cheng and R. X. Zhuo, *Soft Matter*, 2008, 4, 385–391.
- 17 S. K. Ahn, R. M. Kasi, S. C. Kim, N. Sharma and Y. X. Zhou, *Soft Matter*, 2008, 4, 1151–1157.
- 18 J. H. Holtz and S. A. Asher, *Nature*, 1997, 389, 829–832.
- 19 P. S. Stayton, T. Shimoboji, C. Long, A. Chilkoti, G. H. Chen, J. M. Harris and A. S. Hoffman, *Nature*, 1995, 378, 472–474.
- 20 G. J. Randolph, K. Inaba, D. F. Robbani, R. M. Steinman and W. A. Muller, *Immunity*, 1999, 11, 753–761.
- 21 M. Keerl, V. Smirnovas, R. Winter and W. Richtering, *Angew. Chem., Int. Ed.*, 2008, 47, 338–341.
- 22 Y. Hirashima, H. Sato and A. Suzuki, *Macromolecules*, 2005, 38, 9280–9286.
- 23 M. M. Bradford, *Anal. Biochem.*, 1976, 72, 248–254.
- 24 Y. Gonnissen, J. P. Remon and C. Vervaet, *Eur. J. Pharm. Biopharm.*, 2007, 67, 220–226.
- 25 Y. Gonnissen, J. P. Remon and C. Vervaet, *Eur. J. Pharm. Biopharm.*, 2008, 68, 277–282.

26 O. Soga, C. F. van Nostrum and W. E. Hennink, *Biomacromolecules*, 2004, 5, 818–821.